MOLECULAR IMAGING AND BIOLOGY

Mol Imaging Biol (2019) 21:538–548
DOI: 10.1007/s11307-018-1277-9

Published Online: 14 September 2018

RESEARCH ARTICLE

Predictive Value of [^{18}F]ML-10 PET/CT in Early Response Evaluation of Combination Radiotherapy with Cetuximab on Nasopharyngeal Carcinoma

Bingxin Gu,[1,2,3,4,5] Shuai Liu,[1,2,3,4,5] Yuyun Sun,[1,2,3,4,5] Jianping Zhang,[1,2,3,4,5] Yongping Zhang,[1,2,3,4,5] Xiaoping Xu,[1,2,3,4,5] Huiyu Yuan,[1,2,3,4,5] Mingwei Wang,[1,2,3,4,5] Yingjian Zhang,[1,2,3,4,5] Zhongyi Yang[1,2,3,4,5]

[1]*Department of Nuclear Medicine, Fudan University Shanghai Cancer Center, No. 270, Dong'an Road, Xuhui District, Shanghai, China*
[2]*Department of Oncology, Shanghai Medical College, Fudan University, Shanghai, China*
[3]*Center for Biomedical Imaging, Fudan University, Shanghai, China*
[4]*Shanghai Engineering Research Center of Molecular Imaging Probes, Shanghai, China*
[5]*Key Laboratory of Nuclear Physics and Ion-beam Application (MOE), Fudan University, Shanghai, China*

Abstract

Purpose: Apoptosis may be an indication of success therapy, and precise detection of apoptosis can provide instructional suggestions in the therapy management of malignant tumors.

Procedures: We used CNE-1 cell lines for *in vitro* experiments, and colony formation assay, CCK-8 assay, cell apoptosis analysis, and western blotting were performed. For *in vivo* experiments, subcutaneous xenotransplanted tumor models of CNE-1 in nude mice were established. Then, small animal positron emission tomography/X-ray computed tomography (PET/CT) images were acquired by tail intravenous injection of 2-(5-[^{18}F]fluoropentyl)-2-methyl-malonic acid ([^{18}F]ML-10) or 2-deoxy-2-[^{18}F]fluoro-D-glucose ([^{18}F]FDG) before and 24 h and 48 h after treatment. Moreover, expression of epidermal growth factor receptor (EGFR), Ki-67, Glut-1, and terminal deoxynucleotidyl transferase-mediated dUTP nick end labeling (TUNEL) was examined by immunohistochemical examination. Tumor volumes of mice were recorded every 2 days.

Results: In the presence of Cetuximab, the number of colonies of CNE-1 cells decreased significantly after irradiation at 1 and 2 Gy. In addition, Cetuximab increased the radiation-induced cytotoxicity and apoptosis of CNE-1 cells. Mechanistic studies demonstrated that Cetuximab enhanced radiosensitivity by suppressing the EGFR/PI3-K/AKT pathway. In PET/CT imaging, the tumors showed clear uptake of [^{18}F]ML-10 at 24 h and 48 h after combined treatment, and the value of tumor/muscle (T/M) and SUV_{max} (the max of standard uptake value) was significantly higher than those of the other three groups. The T/M of [^{18}F]ML-10 uptake showed a positive correlation of 0.926 with the apoptosis index ($P < 0.001$). However, the uptake of [^{18}F]FDG in tumors exhibited no trend among the four groups. The T/M of [^{18}F]FDG revealed a positive correlation of 0.926 with Glut-1 intensity ($P < 0.001$).

Conclusions: Our work revealed that Cetuximab could increase the radiosensitivity of

Bingxin Gu and Shuai Liu contributed equally to this work.
Electronic supplementary material The online version of this article (https://doi.org/10.1007/s11307-018-1277-9) contains supplementary material, which is available to authorized users.

Correspondence to: Zhongyi Yang; *e-mail:* yangzhongyi21@163.com

CNE-1 cells both *in vitro* and *in vivo*. Apoptosis imaging with [18F]ML-10 PET/CT is a promising modality for application in the response prediction of nasopharyngeal carcinoma.

Key words: Nasopharyngeal carcinoma, Positron emission tomography, CNE-1 cells, Radiotherapy sensitivity, Epidermal growth factor receptor

Introduction

Nasopharyngeal carcinoma (NPC), a geographically heterogeneous disease with the highest incidence rates in southeastern Asia, has become the sixth most common cancer among males in this region [1]. Due to specific biological behavior and anatomic characteristics, radiotherapy is the primary and preferred treatment for NPC [2]. However, given that the rates of locoregional failure and distant failure are 18 % and 22 %, respectively [3], effective treatment remains a challenging issue in future studies.

Recently, attention has been drawn to the inhibition of epidermal growth factor receptor (EGFR) in patients with NPC. EGFR, a type I receptor tyrosine kinases (RTK), plays a crucial role in cell proliferation, migration, and differentiation. It is bound to a growth factor ligand, resulting in dimerization and activation of downstream signaling pathways, including PI3-K/AKT [4]. EGFR is expressed in more than 85 % of NPC, and its overexpression often indicates poor prognosis, early metastasis, or shorter survival [5]. Cetuximab, an anti-EGFR monoclonal antibody, has been approved by both the FDA and EMA as a targeted drug for treatment of head and neck squamous cell carcinomas. Several phase II studies [6–8] have demonstrated the clinical efficacy of Cetuximab in NPC patients. However, not every patient can benefit from it. Thus, early response prediction is crucial in treatment decision.

Positron emission tomography (PET), a noninvasive diagnostic modality, has broadly been applied in early diagnosis, staging, and response evaluation of tumors due to its capacity of monitoring at the cellular level. 2-Deoxy-2-[^{18}F]fluoro-D-glucose ([^{18}F]FDG), routinely used in clinical, could not differentiate tumor and inflammation by reflecting the glucose metabolism state sometimes. 2-(5-[^{18}F]fluoropentyl)-2-methyl-malonic acid ([^{18}F]ML-10), a small molecular probe selectively aggregating in cytoplasm of apoptotic cells, could reveal the degree of apoptosis accurately *in vivo* [9]. Since its absence in inflammatory and necrotic cells, [^{18}F]ML-10 is a potent radiotracer for response prediction early in solid tumors.

Herein, we chose the human nasopharyngeal carcinoma cell line CNE-1, which is not sensitive to radiotherapy, to investigate the radiosensitization effect of Cetuximab *in vitro* and *in vivo*. Furthermore, we demonstrate the utility of [^{18}F]ML-10 PET/CT in xenografts imaging, thus highlighting the potential value of early predicting efficacy of treatment.

Materials and Methods

Materials

[^{18}F]FDG was produced automatically by a cyclotron (Siemens CTI RDS Eclips ST, Knoxville, TN) using the Explora FDG_4 module in our center. Radiolabeling of ML-10 with ^{18}F was synthesized in our center according to the method described by Wang et al. [10]. The radiochemical purity of [^{18}F]FDG and [^{18}F]ML-10 was all more than 95 %.

Cell Lines and CNE-1 Tumor-Bearing Mice Model

The clones of human nasopharyngeal carcinoma cell line CNE-1 were maintained in our laboratory and cultured in Dulbecco's modified Eagle's medium (DMEM) supplemented with penicillin (100 U/ml), streptomycin (100 µg/ml), 10 % fetal bovine serum (FBS), and 2 mM L-glutamine (all from Gibco BRL, Life Technologies, Rockville, MD, USA) in a humidified atmosphere that contained 5 % CO_2 at 37 °C.

Female Balb/c nude mice (4–5 weeks) of 18–20 g body weight were purchased from Lingchang Inst Biotech (Shanghai, China). Tumor xenografts were generated by the subcutaneous injection of CNE-1 cells (1×10^6) in the right hind legs of mice. When the tumor volumes reached 150–300 mm^3, the *in vivo* experiments were carried out.

Colony Formation Assay

For colony formation assay, CNE-1 cells were seeded in 6-well plates at a density of 1×10^3 per well. After 12 h of pre-incubation, the cells were irradiated at 0, 0.5, 1, and 2 Gy with or without Cetuximab (50 µg/ml). Then, the cells were cultured for another 10–14 days. Finally, the cells were washed with phosphate-buffered saline (PBS), fixed with 75 % ethanol, and stained with 0.5 % (*w*/*v*) crystal violet solution. The dishes were photographed, and the colonies with more than 50 cells were counted by microscope (Leica Microsystems, Wetzlar, Germany).

Cell Viability Assay

Cell viability was determined by the CCK-8 assay. The CNE-1 cells were seeded in 96-well plates at a density of

5×10^3 per well (6 wells per group) and allowed to adhere to the plate overnight. After irradiation at 0, 0.5, 1, and 2 Gy with or without Cetuximab (50 μg/ml), the cells were further maintained for 0, 24, 48, 72, and 96 h. One hour before the treatment finished, 10 μl of CCK-8 (Beyotime, Shanghai, China) was added to each well. The absorbance value of each well was measured at 450 nm.

Cell Apoptosis Analysis

PE Annexin V and 7-amino-actinomycin D (7-ADD) were used to detect the cell populations in the apoptosis stage, including the early apoptotic cells and the late apoptotic cells. For the induction of apoptosis, CNE-1 cells were seeded in 6-well plates and then incubated for 24 h after irradiation at 1 Gy with or without Cetuximab (50 μg/ml). The control group was cultured without any treatment. The cells were routinely trypsinized, rinsed with cold PBS, and resuspended with 50 μl 1× binding buffer solution. After being fixed with 4 % paraformaldehyde, 5 μl of PE Annexin V and 5 μl of 7-ADD (KeyGen, Nanjing, Chin) were added to each tube, mixed well, and incubated in the dark for 15 min. Finally, the cells were resuspended with 400 μl of 1× binding buffer. The apoptotic cells were immediately analyzed by using flow cytometry (BD Biosciences, San Jose, CA, USA).

Western Blot Analysis

Treated or untreated CNE-1 cells were washed with PBS, and proteins were extracted from cells using radioimmunoprecipitation assay (RIPA) lysis buffer. A bicinchoninic acid (BCA) protein assay was conducted to quantify the protein concentration. The samples were then separated by a 10 % sodium dodecyl sulfate-polyacrylamide gel electrophoresis (SDS-PAGE), and proteins were transferred onto a nitrocellulose membrane. After being blocked with 5 % defatted milk powder solution for 1 h, the membrane was incubated at 4 °C overnight with Tris-buffered saline containing anti-PI3-K, anti-P-PI3-K, anti-AKT, anti-P-AKT antibody (CST, Danvers), or anti-glyceraldehyde-3-phosphate dehydrogenase (GAPDH) antibody at 1:1000 dilution and then incubated with goat anti-rabbit IgG (H + L) horseradish peroxidase (HRP)-conjugated secondary antibody (diluted 1:5000) for 1 h at room temperature. The immunostained membranes were visualized with a Chemidoc XRS imaging system (Bio-Rad, Laboratories, Inc.). The results were normalized to GAPDH to correct for loading.

In vivo PET/CT Imaging

In vivo PET/CT imaging scans and image analysis were performed using an Inveon Animal-PET/CT (Siemens Preclinical Solution, Knoxville, TN). Mice ($n = 3$) with subcutaneous CNE-1 xenografts were scanned 1 h after injection of radiolabeled tracer (*via* tail vein with 5.55 MBq [^{18}F]FDG or [^{18}F]ML-10 in 0.2 ml saline) before and 24 h and 48 h after irradiation (15 Gy per mouse) with or without Cetuximab (1 mg per mouse). During scanning, the mice were maintained with anesthetization using 2.5 % isoflurane/oxygen. In addition, mice in the [^{18}F]FDG groups were fasted 4 h before tracer injection. Mice without any treatment were used as controls. While raw images were acquired, the three-dimensional ordered-subset expectation maximization (OSEM3D)/maximum algorithm was used for image reconstruction. The max of percentage-injected dose per gram (%ID/g_{max}) and standard uptake value (SUV_{max}) of the tumor was measured by manually drawn region of interest (ROI). The %ID/g_{max} of the opposite hind leg muscle was used as background. The T/M was calculated according to the formula T/M = tumor (%ID/g_{max}) / muscle (%ID/g_{max}).

Following the imaging, mouse weights and tumor volumes were continuously recorded for 1 month. The volume of the xenograft was expressed as $V = ab^2/2$, where V is the volume of the xenograft, a is the long diameter of the xenograft, and b is the short diameter of the xenograft.

Immunohistochemical Examination

Mice ($n = 3$) were euthanized before and 24 h and 48 h after treatment, and tumor tissues were collected, fixed in formalin, and embedded in paraffin immediately. The tumor samples were sectioned at a thickness of 5 mm and deparaffinized, rehydrated, and heated for antigen retrieval. Endogenous peroxidase was deactivated by incubating the slides in 3 % H_2O_2 for 10 min. The sections were then blocked with 10 % normal goat serum for 10 min and further incubated with a primary mouse anti-EGFR antibody, a monoclonal mouse anti-Glut-1 antibody or a monoclonal rabbit anti-Ki-67 antibody (Abcam, UK) at 4 °C overnight. The apoptotic cell identification was performed using the terminal deoxynucleotidyl transferase-mediated dUTP nick end labeling (TUNEL) technique with a cell death detection kit. Then, the slides were incubated with a broad-spectrum secondary antibody conjugated with HRP, treated with diaminobenzidine (DAB), and counterstained with hematoxylin before mounting. Untreated sections without any antibody were used as negative controls. Integrated optical density (IOD) of images was measured for semiquantitative analysis.

Statistical Analysis

Data were statistically analyzed using SPSS 20.0 (SPSS Inc., Chicago, IL, USA) and expressed as the mean ± standard deviation (SD). All experiments were performed at least in triplicate. Significant differences in the mean values were evaluated using Student's unpaired t test. Where multiple comparisons were required, analysis was

performed using two-way analysis of variance with Bonferroni correction. Pearson correlation r was used to calculate the correlations between T/M and immunohistochemistry. $P < 0.05$ was considered to indicate a statistically significant difference.

Results

Cetuximab Decreases the Colony Formation in CNE-1 Cell Cultures Exposed to Radiation

CNE-1 cells were exposed to different radiation doses (0, 0.5, 1, and 2 Gy) with pretreatment with or without Cetuximab (50 μg/ml) to determine colony formation. As shown in Fig. 1, there were significantly decreased colony numbers in the Cetuximab + radiation group compared with the radiation only group. In the presence of Cetuximab, there was a statistically significant difference in the colonies of the combination treatment group compared with control group once the radiation dose increased to 1 Gy. Additionally, there was also a significant difference between the combined treatment group and the radiation group, though the number of colonies in the radiation group was clearly reduced with radiation at 2 Gy.

Cetuximab Increased the Cytotoxicity of CNE-1 Cells Exposed to Radiation

The inhibitory effects of Cetuximab (50 μg/ml) on the proliferation of CNE-1 cells irradiated at different doses (0, 0.5, 1 and 2 Gy) were detected by using a CCK-8 kit. As presented in Suppl. Fig. 1 (see electronic supplemental material: ESM), Cetuximab caused significant suppression of the proliferation of CNE-1 cells when combined with radiation compared with those in the radiation only and control groups at 24, 48, 72, and 96 h.

Cetuximab Promotes CNE-1 Cell Apoptosis upon Exposure to Radiation

The effects of radiation on the apoptosis of CNE-1 cells treated with or without Cetuximab were detected by Annexin V and 7-ADD. As shown in Fig. 2, untreated cells in the control, radiation, and Cetuximab + radiation groups exhibited apoptosis rates of 3.70 ± 0.20, 8.23 ± 0.95, and 10.77 ± 0.49 %, respectively. The data showed that irradiation exposure significantly induced apoptotic events compared with the blank control cells. Furthermore, the percentage of apoptosis in the combination treatment group was significantly higher than that in the radiation group.

Cetuximab Increases the Radiotherapy Sensitivity by Suppressing PI3-K/AKT Signaling

To gain insight into the mechanism by which Cetuximab restores the radiotherapy sensitivity to CNE-1 cells, we examined the expression of proteins related to EGFR signaling (PI3-K/AKT) by western blotting. Figure 3 and Suppl. Fig. 2 (see ESM) show that the P-PI3-K and P-AKT levels were obviously downregulated in the Cetuximab + radiation group compared to radiation group, while the opposite trend was observed for PI3-K and AKT levels. In the presence of PI3-K inhibitor, similar results were obtained. The results indicated that Cetuximab increases the radiotherapy sensitivity by decreasing the phosphorylation level of PI3-K/AKT.

[^{18}F]ML-10 PET/CT Imaging Predicts Response to Treatment Early

To evaluate the apoptosis conditions of xenografts irradiated (15 Gy per mouse) with or without Cetuximab (1 mg per mouse) *in vivo*, PET/CT images of tumor-bearing mice were acquired before as well as 24 h and 48 h after treatment by utilizing [^{18}F]ML-10. As presented in Fig. 4a, the tumor regions in the four groups showed extremely low radioactivity before treatment, which was close to that of muscle. After being treated with radiation and Cetuximab for 24 h and 48 h, the radioactive uptake increased significantly in tumors, while the other groups treated with radiation or Cetuximab alone remained at a low radioactivity. The value of T/M (Fig. 4b) showed no significant difference among the four groups before treatment. Furthermore, the T/M of Cetuximab + radiation group increased significantly ($P < 0.05$) compared with radiation, Cetuximab, and control groups at both 24 h (9.50 ± 5.78, 2.83 ± 0.29, 1.29 ± 0.13 and 1.16 ± 0.14, respectively) and 48 h (9.18 ± 3.36, 2.34 ± 0.53, 3.11 ± 0.15 and 1.23 ± 0.24, respectively) after treatment. The value of SUV_{max} (Fig. 4c) showed the same trend as T/M ($P < 0.05$). The tumor volume changes of the four groups are exhibited in Suppl. Fig. 3 (see ESM). As expected, the volume of tumors in the combination treatment group decreased significantly, while it increased gradually in other groups after treatment. The results suggested that Cetuximab could increase radiotherapy sensitivity of CNE-1 xenograft *in vivo*, and [^{18}F]ML-10 PET/CT imaging could predict response to treatment early *via* change in T/M and SUV_{max}.

[^{18}F]FDG PET/CT Imaging Is Limited to Predict Response to Treatment

The glucose metabolism of tumors was monitored *in vivo* by [^{18}F]FDG PET/CT imaging. As shown in Fig. 5a, the tumor regions in the four groups showed high radioactivity before and 24 h and 48 h after treatment. However, there were no

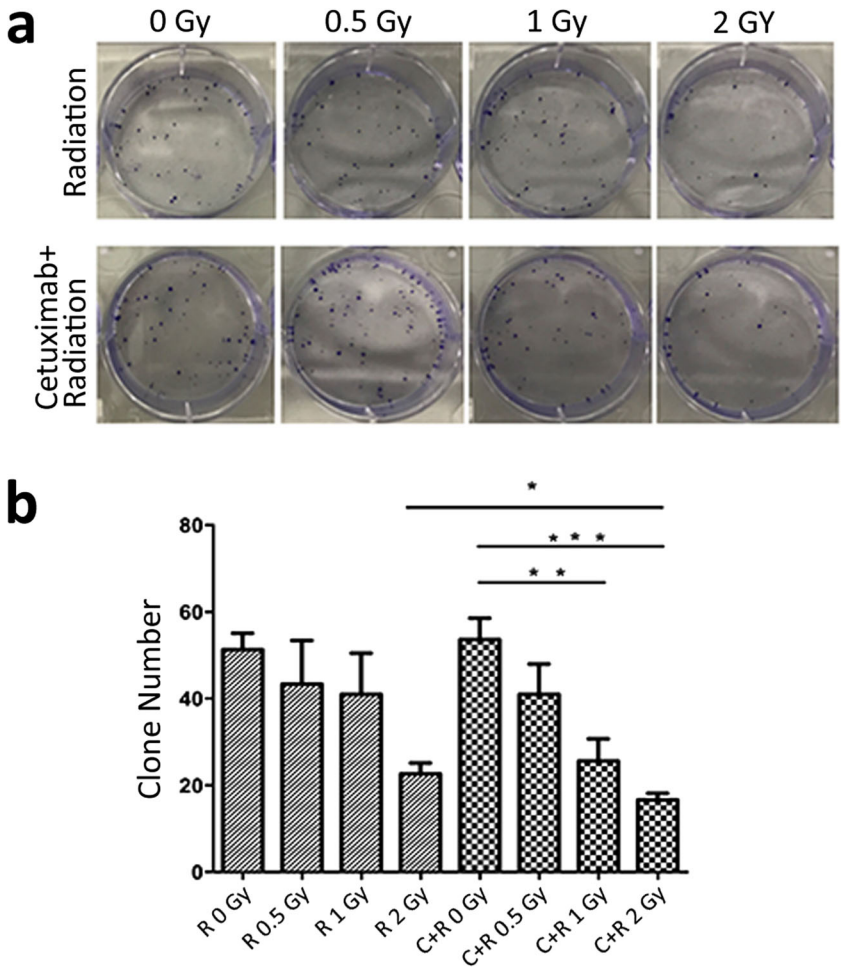

Fig. 1. Effect of combined radiation with Cetuximab on colony formation in CNE-1 cells. **a** Photographs of colony formation on dishes. Cells were irradiated at 0, 0.5, 1, and 2 Gy with 50 μg/ml of Cetuximab (lower) or not (upper). **b** Quantitative analysis of colony formation. The error bars shown in the figure represent the mean ± SD ($n = 3$ independent experiments). Differences were determined with Student's unpaired t test, $^{*}P < 0.05$, $^{**}P < 0.01$, and $^{***}P < 0.001$ indicate significant differences between C + R 2 Gy and R 2 Gy, C + R 1 Gy and C + R 0 Gy, and C + R 2 Gy and C + R 0 Gy, respectively.

significant differences among these groups in the value of T/M (Fig. 5b) and SUV_{max} (Fig. 5c) in spite of treatment. The results demonstrated that radiation or Cetuximab does not affect the CNE-1 xenograft glucose metabolism.

Cetuximab + Radiation Inhibits EGFR Expression In Vivo

The variation trends of EGFR expression in CNE-1 xenografts with different treatments were examined by immunohistochemical examination. The staining results (Suppl. Fig. 4; see ESM) showed that compared with the radiation, Cetuximab, and control groups, Cetuximab + radiation treatment clearly decreased EGFR expression in CNE-1 tumors, though no significant differences were observed at 24 h. The result suggested that Cetuximab increases the radiotherapy sensitivity by suppressing the expression of EGFR.

Cetuximab + Radiation Suppresses Cell Proliferation In Vivo

The proliferation of CNE-1 xenograft was determined by Ki-67 assay. As shown in Suppl. Fig. 5 (see ESM), Ki-67 intensity was significantly decreased in the Cetuximab + radiation group compared with the radiation and control groups at 24 h and 48 h. Though there was no significant difference between the Cetuximab + radiation and Cetuximab groups, the Ki-67 intensity was much less than that in the prior group. The data indicated that a combination of Cetuximab with radiation could inhibit xenograft proliferation *in vivo*.

Cetuximab + Radiation Induces Apoptosis In Vivo and [18F]ML-10 Uptake Correlated Well with TUNEL

TUNEL assay was performed to observe the apoptotic cells in the tumors. As presented in Fig. 6a, b, there were more

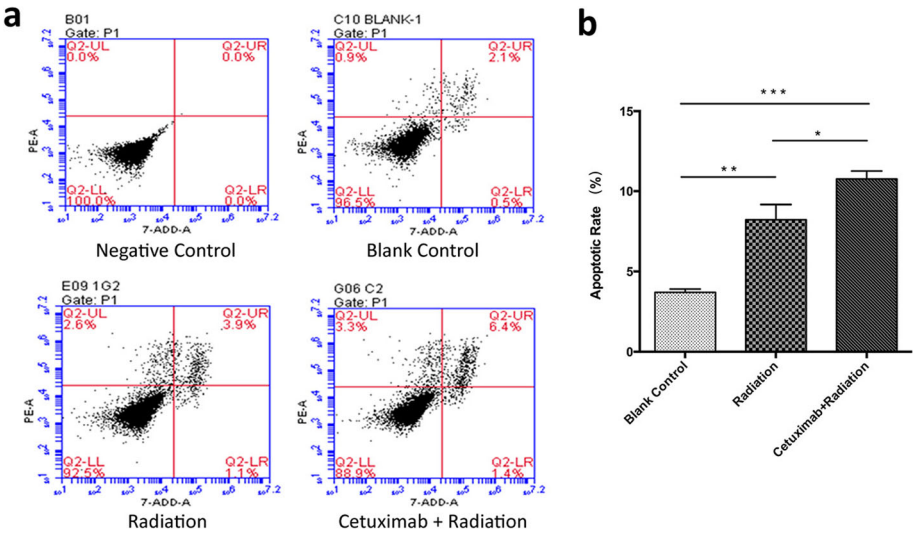

Fig. 2. Effect of combined radiation with Cetuximab on apoptosis of CNE-1 cells. **a** Representative figures of flow cytometry results. **b** Quantitative analysis of apoptotic rates. Flow cytometric analysis was carried out in CNE-1 cells treated with negative control, blank control, radiation (1 Gy), and Cetuximab (50 μg/ml) plus radiation (1 Gy) at 24 h after cells were seeded. The error bars shown in the figure represent the mean ± SD ($n = 3$ independent experiments). Differences were determined with Student's unpaired t test, $^{*}P < 0.05$, $^{**}P < 0.01$, $^{***}P < 0.001$.

TUNEL-positive cells in the Cetuximab + radiation group than in the radiation, Cetuximab, and control groups, indicating that Cetuximab increased apoptosis of CNE-1 xenografts in the presence of radiation. The T/M of

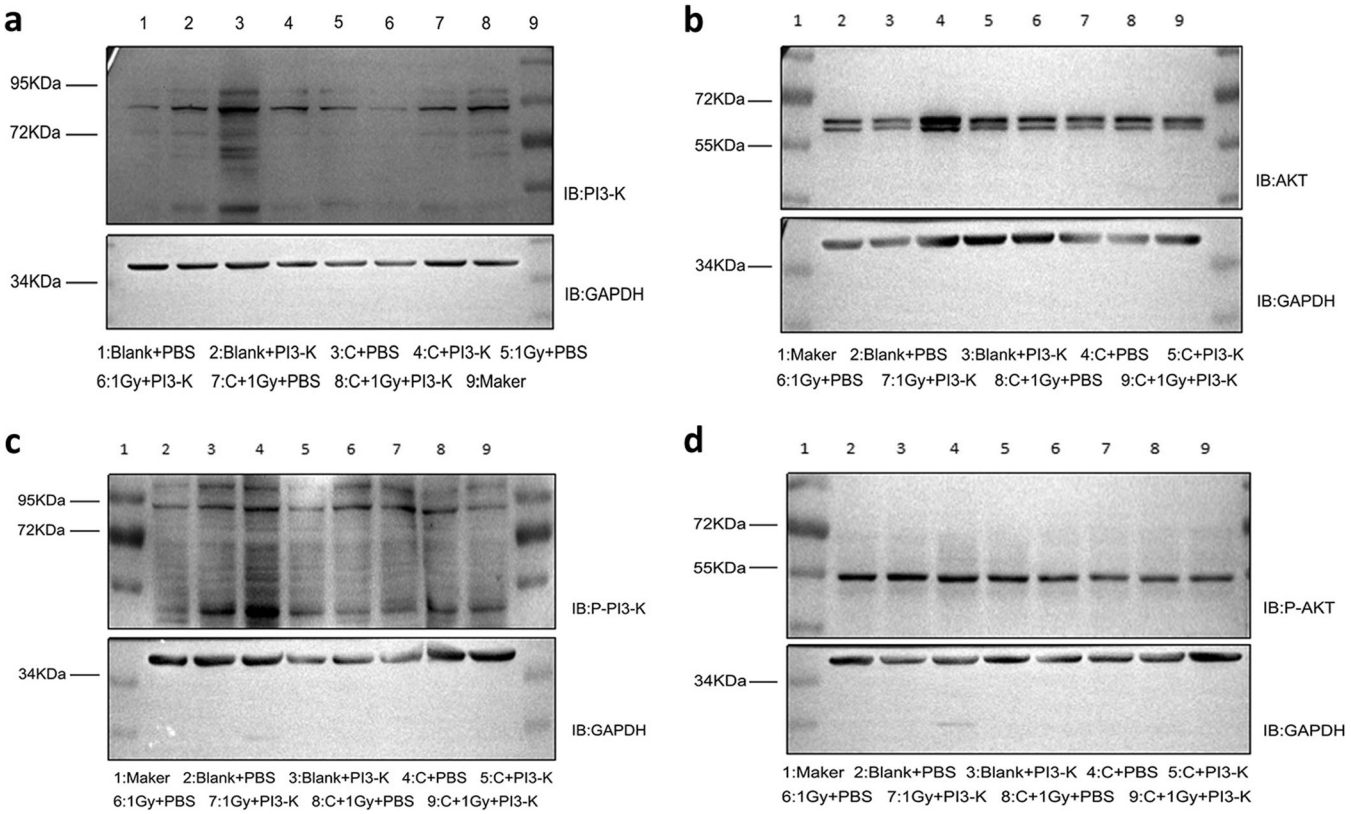

Fig. 3. Expression level of proteins in CNE-1 cells. **a** PI3-K. **b** AKT. **c** P-PI3-K. **d** P-AKT. Cells were treated with control, Cetuximab (50 μg/ml), radiation (1 Gy), and Cetuximab (50 μg/ml) plus radiation (1 Gy) in the presence of PI3-K inhibitor or not. Expression level of these proteins was then determined by western blot analysis. GAPDH was used as a loading control.

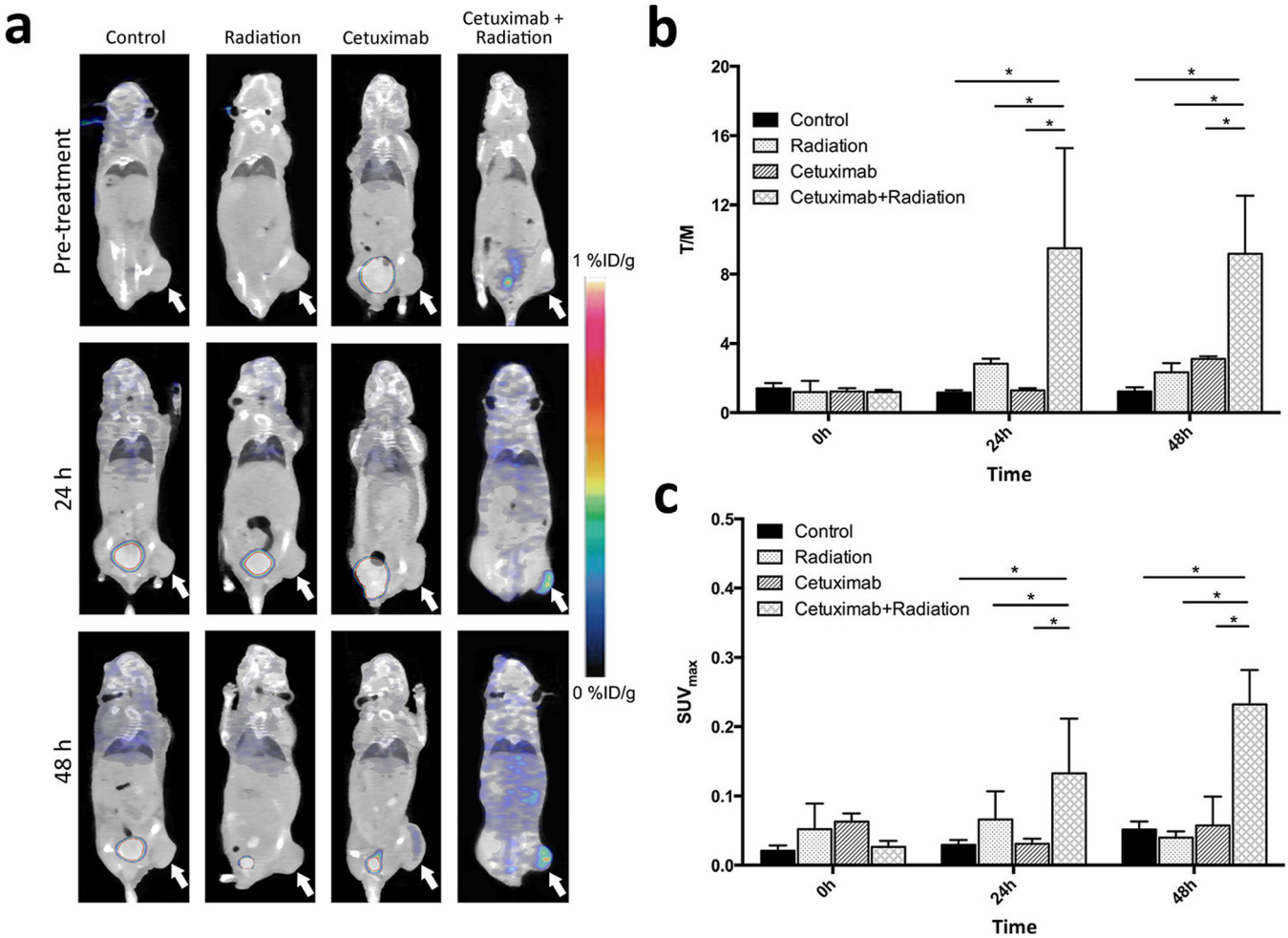

Fig. 4. *In vivo* imaging analysis of [18F]ML-10 PET/CT. **a** Representative whole-body coronal [18F]ML-10 PET/CT images of subcutaneous CNE-1 xenografts before and 24 h and 48 h after irradiation (15 Gy/mouse), Cetuximab (1 mg/mouse), or Cetuximab (1 mg/mouse) plus irradiation (15 Gy/mouse). Mice without any treatment used as control. White arrow shows location of tumors. **b**, **c** Quantitative analysis of the PET/CT images. T/M was calculated according to the formula T/M = tumor (%ID/g_{max}) / muscle (%ID/g_{max}). The error bars shown in the figure represent the mean ± SD ($n = 5$ independent experiments). Statistical analysis was determined with two-way ANOVA, $^*P < 0.05$.

[18F]ML-10 and apoptosis index revealed a positive correlation of 0.926 (Fig. 6c, $P < 0.001$).

[18F]FDG Uptakes Correlated Well with Glut-1

Glut-1 staining was applied to verify glucose metabolism in CNE-1 xenografts. As expected, Glut-1 intensity did not show a clear change in the four groups with or without treatment (Suppl. Fig. 6a, b; see ESM). The T/M of [18F]FDG and Glut-1 intensity revealed a positive correlation of 0.926 (Suppl. Fig. 6c, $P < 0.001$; see ESM).

Discussion

Therapeutic strategies of NPC have changed from conventional radiotherapy to intensity-modulated radiotherapy (IMRT), chemotherapy, or chemoradiotherapy, which could substantially improve the prognosis of locally advanced NPC prominently [11–13]. Though the incidence and mortality of NPC have declined gradually over the past two decades, 92 % of new cases occur in economically less-developed countries, thus heavily increasing their economic burden [14–16]. Furthermore, local recurrence and distant metastasis remain a headache, revealing a poor prognosis with median survival times ranging from only 5 to 11 months [6]. Recently, the molecular targeted therapies have shown potency in heavily pretreated NPC patients. Cetuximab, which selectively inhibits EGFR, is primarily utilized in treatment of colorectal cancer and has been proven to improve response rate in treatment of NPC. In a previous study of Cetuximab in patients with stage III/IV nasopharyngeal carcinoma, measurable complete responses were recorded in 84 % of individuals, with 72 % showing 3-year

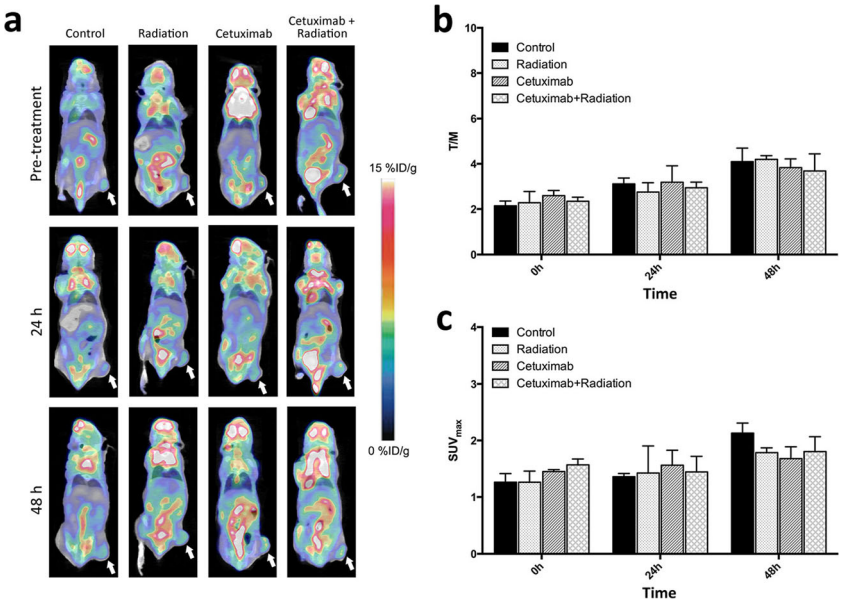

Fig. 5. *In vivo* imaging analysis of [18F]FDG PET/CT. **a** Representative whole-body coronal [18F]FDG PET/CT images of subcutaneous CNE-1 xenografts before and 24 h and 48 h after irradiation (15 Gy/mouse), Cetuximab (1 mg/mouse), or Cetuximab (1 mg/mouse) plus irradiation (15 Gy/mouse). Mice without any treatment used as control. White arrow shows location of tumors. **b**, **c** Quantitative analysis of the PET/CT images. The value of T/M and SUV_{max} in combination group showed no significant difference compared with control, radiation, and Cetuximab groups at 0 h, 24 h, and 48 h.

local regional control [8]. Our results corroborate the effective of Cetuximab in combination treatment of nasopharyngeal carcinoma *in vitro* and *in vivo*.

EGFR has been reported to be an independent predictor of clinical outcome in NPC, where high expression indicates poor prognosis [17, 18]. The anti-tumor mechanisms of Cetuximab have been revealed to include blocking the EGFR downstream signal by competitive inhibition of ligand binding, downregulation of the expression of EGFR through dimerization and internalization, and facilitation of antibody-dependent cell-mediated cytotoxicity (ADCC) [19]. It is well known that the three main pathways downstream of EGFR are the PI3-K/AKT, JAK/STAT, and Ras/Raf pathways [20]. In this work, we explored the correlation of EGFR/PI3-K/AKT signaling with radiosensitization in CNE-1 cells. Our data revealed that EGFR protein expression was markedly decreased with treatment of Cetuximab combined with radiotherapy *in vivo*. In addition to downregulating EGFR expression, Cetuximab was also observed to decrease the phosphorylation of PI3-K and AKT, thereby blocking the signal transduction and resulting in apoptosis as well as proliferation suppression in CNE-1 cells. This is supported by previous studies, which demonstrated that the PI3-K/AKT pathway is related to radioresistance and that blocking the PI3-K/AKT signaling *via* EGFR inhibition can sensitize NPC cells to radiation [21–23]. As expected, we observed that cell proliferation was significantly inhibited by treatment with Cetuximab plus radiotherapy. Furthermore, radiotherapy reduced the formation of colonies of CNE-1 cells in the presence of Cetuximab compared with radiation or Cetuximab alone. In addition, Cetuximab dramatically increased the radiation-induced apoptosis rate as measured by flow cytometry assay as well as the TUNEL assay. Notably, the Cetuximab treatment alone had no significant effect on growth of CNE-1 cells both *in vitro* and *in vivo*, similar to a report by SUNG et al. [24], which suggested that Cetuximab enforced its anti-tumor effect in a synergistic manner. Taken together, these data indicated that Cetuximab may increase the radiosensitivity of CNE-1 cells by suppressing EGFR-signaling *via* inactivating the PI3-K/AKT-pathway.

Currently, to realize personalized treatment, increasing attention has focused on molecular imaging, which could characterize and measure the processes of tumor progression *in vivo* at cellular and molecular level [25]. PET is one of the molecular imaging modalities. With the various positron-labeled tracer applications, PET could provide a wealth of information, including that of metabolic [26, 27], proliferation [28], and receptor expression [29]. [18F]ML-10 is a novel member of the Aposense family and aims to sensitively detect the death process from its early stages. Based on the malonate moiety, [18F]ML-10 could selectively cross the plasma membrane and is mainly localized to the cytoplasm (60 %) of apoptotic cells rather than viable cells, thus enabling a high signal/background ratio [30]. Because of the small molecular weight of 206 Da, [18F]ML-10 showed a rapid clearance from blood through kidneys and quick excretion from nontarget organs, resulting in a stable T/M from 30 min after probe administration both in an animal model [9] and in patients [31, 32]. Regarding the aspects of radiolabeling, biodistribution and immunogenicity, [18F]ML-10 is superior to large proteins

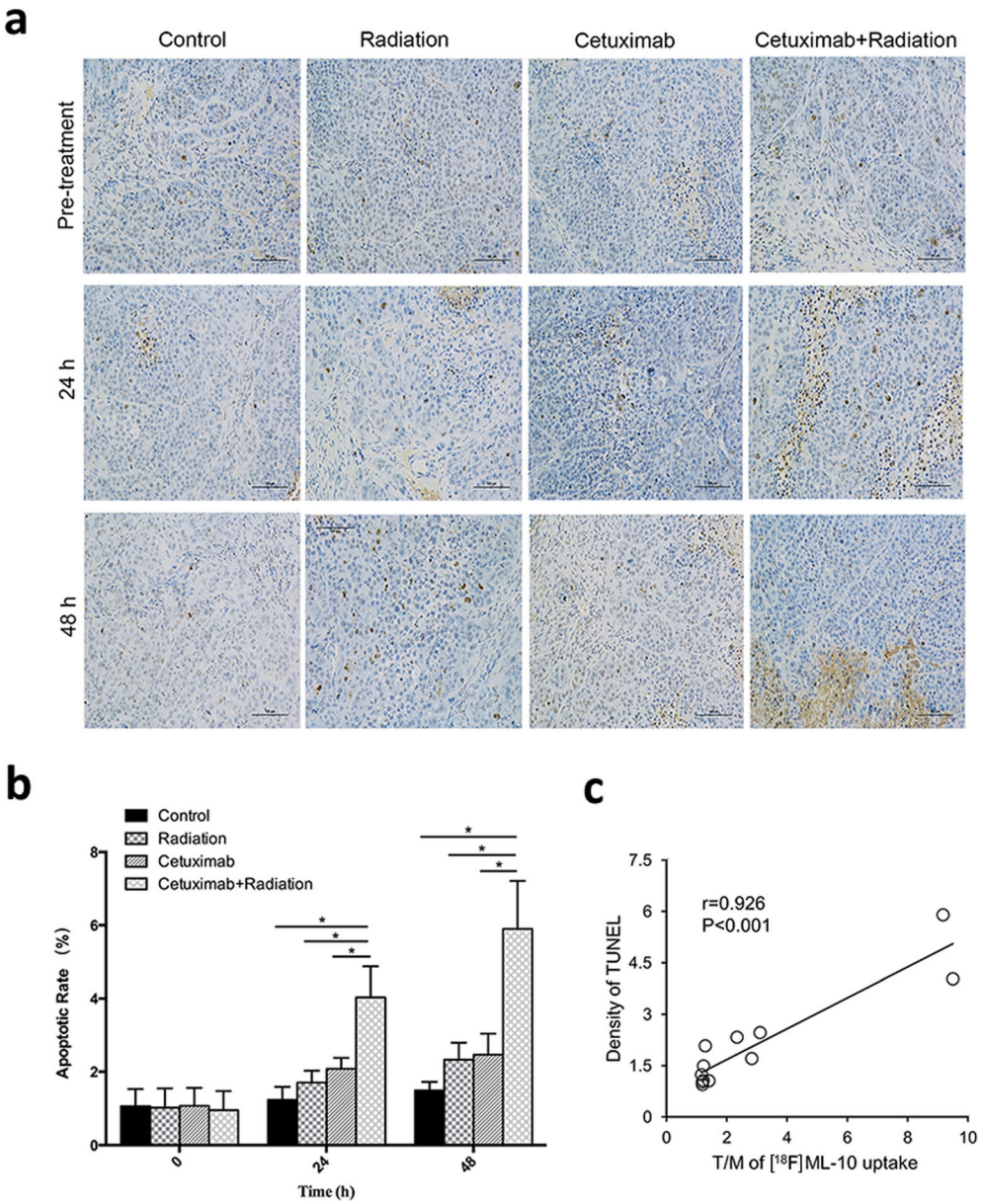

Fig. 6. TUNEL assessment of apoptosis in CNE-1 xenografts. **a** Photomicrographs of tumor sections from control and radiation (15 Gy/mouse), Cetuximab (1 mg/mouse), or Cetuximab (1 mg/mouse) plus radiation (15 Gy/mouse) groups at 0 h, 24 h, and 48 h. Brown shows TUNEL-positive cells, blue shows location of nucleus, and scale bars represent 100 μm in length. **b** Quantitative analysis of apoptotic rate. The error bars shown in the figure represent the mean ± SD ($n = 5$ independent experiments). Statistical analysis was determined with two-way ANOVA, $^*P < 0.05$. **c** Correlation analysis between T/M of [18F]ML-10 uptake and TUNEL-positive density.

such as Annexin-V [33]. Since apoptosis may be an early indication of the success of therapy, detection of apoptosis can potentially provide prognostic information and guide the subsequent treatment regimen [34]. In the first human study [35], Matthew J et al. applied [18F]ML-10 to evaluate the response to radiation in a newly diagnosed glioblastoma multiforme patient by the change in uptake before and quickly after therapy. However, the follow-up information was unavailable.

In our study, we innovatively performed the [18F]ML-10 PET/CT for early prediction of the response to Cetuximab combined with radiotherapy in treatment of CNE-1 xenograft *in vivo*. We found that tumors with apoptotic cells showed high uptake of [18F]ML-10 after combination treatment. In addition, the change in T/M before and after treatment played a role in prediction of response, while the mice with high T/M of [18F]ML-10 at an early time after treatment revealed a better prognosis. The value of T/M showed a good correlation to the intensity of TUNEL, while the latter was the gold standard but invasive. Given the wide application of [18F]FDG in clinical settings [36], we also

investigated the uptake of [18F]FDG in treated CNE-1 xenografts. Unfortunately, the value of T/M fluctuated irregularly in CNE-1 tumors before and after treatment even in the combination treatment group, which was verified by Glut-1 examination.

Conclusion

For the first time, we applied [18F]ML-10 PET/CT to evaluate the response to radiation in the presence of Cetuximab on CNE-1 cells *in vivo*. The change in T/M before and soon after treatment provided reliable prognostic information. Moreover, we investigated the combination efficacy of Cetuximab and radiotherapy on anticancer effects and the molecular mechanism in human NPC lines CNE-1. Our results showed that Cetuximab could increase the radiosensitivity of CNE-1 cells, which may be due to the inhibition of EGFR/PI3-K/AKT-pathway. Wide application of [18F]ML-10 PET/CT in clinical settings may benefit patients, and our work serves as a foundation for that.

Acknowledgements. We wish to thank Jianmin Luo for excellent technical assistances.

Funding Information. This study was funded by the National Natural Science Foundation of China (No. 81501503) and the Shanghai Engineering Research Center of Molecular Imaging Probes Program (No. 14DZ2251400).

Compliance with Ethical Standards. All animal experiments met guidelines evaluated and approved by the ethics committee of Fudan University.

Conflict of Interest

The authors declare that they have no conflict of interest.

Ethical Approval

All applicable institutional and/or national guidelines for the care and use of animals were followed.

References

1. Torre LA, Bray F, Siegel RL, Ferlay J, Lortet-Tieulent J, Jemal A (2015) Global cancer statistics, 2012. CA Cancer J Clin 65:87–108
2. Chua MLK, Wee JTS, Hui EP, Chan ATC (2016) Nasopharyngeal carcinoma. Lancet 387:1012–1024
3. Blanchard P, Lee A, Marguet S, Leclercq J, Ng WT, Ma J, Chan AT, Huang PY, Benhamou E, Zhu G, Chua DT, Chen Y, Mai HQ, Kwong DL, Cheah SL, Moon J, Tung Y, Chi KH, Fountzilas G, Zhang L, Hui EP, Lu TX, Bourhis J, Pignon JP, MAC-NPC Collaborative Group (2015) Chemotherapy and radiotherapy in nasopharyngeal carcinoma: an update of the MAC-NPC meta-analysis. Lancet Oncol 16:645–655
4. Bublil EM, Yarden Y (2007) The EGF receptor family: spearheading a merger of signaling and therapeutics. Curr Opin Cell Biol 19:124–134
5. Zhang P, Wu SK, Wang Y et al (2015) p53, MDM2, eIF4E and EGFR expression in nasopharyngeal carcinoma and their correlation with clinicopathological characteristics and prognosis: a retrospective study. Oncol Lett 9:113–118
6. Chan AT, Hsu MM, Goh BC et al (2005) Multicenter, phase II study of cetuximab in combination with carboplatin in patients with recurrent or metastatic nasopharyngeal carcinoma. J Clin Oncol 23:3568–3576
7. Ma BB, Kam MK, Leung SF et al (2012) A phase II study of concurrent cetuximab-cisplatin and intensity-modulated radiotherapy in locoregionally advanced nasopharyngeal carcinoma. Ann Oncol 23:1287–1292
8. Suntharalingam M, Kwok Y, Goloubeva O, Parekh A, Taylor R, Wolf J, Zimrin A, Strome S, Ord R, Cullen KJ (2012) Phase II study evaluating the addition of cetuximab to the concurrent delivery of weekly carboplatin, paclitaxel, and daily radiotherapy for patients with locally advanced squamous cell carcinomas of the head and neck. Int J Radiat Oncol Biol Phys 82:1845–1850
9. Reshef A, Shirvan A, Waterhouse RN, Grimberg H, Levin G, Cohen A, Ulysse LG, Friedman G, Antoni G, Ziv I (2008) Molecular imaging of neurovascular cell death in experimental cerebral stroke by PET. J Nucl Med 49:1520–1528
10. (2013) Poster Presentation. J Label Compd Radiopharm 56:S88–S462. https://doi.org/10.1002/jlcr.3058
11. Chen QY, Wen YF, Guo L, Liu H, Huang PY, Mo HY, Li NW, Xiang YQ, Luo DH, Qiu F, Sun R, Deng MQ, Chen MY, Hua YJ, Guo X, Cao KJ, Hong MH, Qian CN, Mai HQ (2011) Concurrent chemoradiotherapy vs radiotherapy alone in stage II nasopharyngeal carcinoma: phase III randomized trial. J Natl Cancer Inst 103:1761–1770
12. Lee AW, Ng WT, Chan LL et al (2014) Evolution of treatment for nasopharyngeal cancer—success and setback in the intensity-modulated radiotherapy era. Radiother Oncol 110:377–384
13. Wu X, Huang PY, Peng PJ, Lu LX, Han F, Wu SX, Hou X, Zhao HY, Huang Y, Fang WF, Zhao YY, Xue C, Hu ZH, Zhang J, Zhang JW, Ma YX, Liang WH, Zhao C, Zhang L (2013) Long-term follow-up of a phase III study comparing radiotherapy with or without weekly oxaliplatin for locoregionally advanced nasopharyngeal carcinoma. Ann Oncol 24:2131–2136
14. Lee AW, Foo W, Mang O et al (2003) Changing epidemiology of nasopharyngeal carcinoma in Hong Kong over a 20-year period (1980-99): an encouraging reduction in both incidence and mortality. Int J Cancer 103:680–685
15. Tang LL, Chen WQ, Xue WQ, He YQ, Zheng RS, Zeng YX, Jia WH (2016) Global trends in incidence and mortality of nasopharyngeal carcinoma. Cancer Lett 374:22–30
16. Xu Z-X, Lin Z-X, Fang J-Y, Wu KS, du PL, Zeng Y, Tang WR, Xu XL, Lin K (2015) Mortality characteristic and prediction of nasopharyngeal carcinoma in China from 1991 to 2013. Asian Pac J Cancer Prev 16:6729–6734
17. Chua DTT, Nicholls JM, Sham JST, Au GKH (2004) Prognostic value of epidermal growth factor receptor expression in patients with advanced stage nasopharyngeal carcinoma treated with induction chemotherapy and radiotherapy. Int J Radiat Oncol Biol Phys 59:11–20
18. Ma X, Huang J, Wu X, Li X, Zhang J, Xue L, Li P, Liu L (2014) Epidermal growth factor receptor could play a prognostic role to predict the outcome of nasopharyngeal carcinoma: a meta-analysis. Cancer Biomark 14:267–277
19. Trivedi S, Concha-Benavente F, Srivastava RM, Jie HB, Gibson SP, Schmitt NC, Ferris RL (2015) Immune biomarkers of anti-EGFR monoclonal antibody therapy. Ann Oncol 26:40–47
20. Prenzel N, Fischer OM, Streit S, Hart S, Ullrich A (2001) The epidermal growth factor receptor family as a central element for cellular signal transduction and diversification. Endocr Relat Cancer 8:11–31
21. Bussink J, van der Kogel AJ, Kaanders JHAM (2008) Activation of the PI3-K/AKT pathway and implications for radioresistance mechanisms in head and neck cancer. Lancet Oncol 9:288–296
22. Gu J, Yin L, Wu J, Zhang N, Huang T, Ding K, Cao H, Xu L, He X (2016) Cetuximab and cisplatin show different combination effect in nasopharyngeal carcinoma cells lines via inactivation of EGFR/AKT signaling pathway. Biochem Res Int 2016:7016907
23. Stegeman H, Kaanders JH, van der Kogel AJ, Iida M, Wheeler DL, Span PN, Bussink J (2013) Predictive value of hypoxia, proliferation and tyrosine kinase receptors for EGFR-inhibition and radiotherapy sensitivity in head and neck cancer models. Radiother Oncol 106:383–389
24. Sung FL, Poon TCW, Hui EP et al (2005) Antitumor effect and enhancement of cytotoxic drug activity by cetuximab in nasopharyngeal carcinoma cells. In Vivo 19:237–245
25. Ralph W, Umar M (2001) Molecular imaging. Radiology 219:316–333

26. Hatt M, Majdoub M, Vallieres M et al (2014) ^{18}F-FDG PET uptake characterization through texture analysis: investigating the complementary nature of heterogeneity and functional tumor volume in a multi-cancer site patient cohort. J Nucl Med 56:38–44
27. Oyama N, Miller TR, Dehdashti F et al (2003) ^{11}C-acetate PET imaging of prostate cancer: detection of recurrent disease at PSA relapse. J Nucl Med 44:549–555
28. Chen W, Cloughesy T, Kamdar N, Satyamurthy N, Bergsneider M, Liau L, Mischel P, Czernin J, Phelps ME, Silverman DH (2005) Imaging proliferation in brain tumors with ^{18}F-FLT PET: comparison with ^{18}F-FDG. J Nucl Med 46:945–952
29. Linden HM, Stekhova SA, Link JM, Gralow JR, Livingston RB, Ellis GK, Petra PH, Peterson LM, Schubert EK, Dunnwald LK, Krohn KA, Mankoff DA (2006) Quantitative fluoroestradiol positron emission tomography imaging predicts response to endocrine treatment in breast cancer. J Clin Oncol 24:2793–2799
30. Cohen A, Shirvan A, Levin G (2009) From the Gla domain to a novel small-molecule detector of apoptosis. Cell Res 19:625–637
31. Hoglund J, Shirvan A, Antoni G, Gustavsson SA, Langstrom B, Ringheim A, Sorensen J, Ben-Ami M, Ziv I (2011) ^{18}F-ML-10, a PET tracer for apoptosis: first human study. J Nucl Med 52:720–725
32. Oborski MJ, Laymon CM, Qian Y, Lieberman FS, Nelson AD, Mountz JM (2014) Challenges and approaches to quantitative therapy response assessment in glioblastoma multiforme using the novel apoptosis positron emission tomography tracer F-18 ML-10. Transl Oncol 7:111–119
33. De Saint-Hubert M, Prinsen K, Mortelmans L et al (2009) Molecular imaging of cell death. Methods 48:178–187
34. Neves AA, Brindle KM (2006) Assessing responses to cancer therapy using molecular imaging. Biochim Biophys Acta 1766:242–261
35. Oborski MJ, Laymon CM, Lieberman FS, Drappatz J, Hamilton RL, Mountz JM (2014) First use of ^{18}F-labeled ML-10 PET to assess apoptosis change in a newly diagnosed glioblastoma multiforme patient before and early after therapy. Brain Behav 4:312–315
36. Shankar LK, Hoffman JM, Bacharach S, Graham MM, Karp J, Lammertsma AA, Larson S, Mankoff DA, Siegel BA, van den Abbeele A, Yap J, Sullivan D, National Cancer Institute (2006) Consensus recommendations for the use of ^{18}F-FDG PET as an indicator of therapeutic response in patients in National Cancer Institute trials. J Nucl Med 47:1059–1066